Presented at the 26th European PV Solar Energy Conference and Exhibition, 5-9 September 2011, Hamburg, Germany

LASER MARKING OF SOLAR CELLS: TECHNOLOGIES AND POTENTIAL

A. Krieg, N. Rajsrima, S. Rein
Fraunhofer Institute for Solar Energy Systems (ISE)
Heidenhofstrasse 2, 79110 Freiburg, Germany
Phone: +49-761-4588-5488, Fax: +49-761-4588-9250, Email: alexander.krieg@ise.fraunhofer.de

ABSTRACT: In this work, laser marking processes for wafer identification have been investigated on mono-crystalline silicon wafers with respect to the laser-induced damage using small Data Matrix codes with a code size of 0.8 x 3.2 mm² and a brick slice code. The experiment focuses on the identification of shunts, the breakdown characteristics and the recombination losses of Al BSF solar cells to check if a purely geometric specification of a front-side marking is sufficient for the ongoing standardization procedure. The analysis of photoluminescence images shows that recombination losses which affect the finished solar cell are only detectable after ARC. Thermography revealed that a severe hot spot risk only arises for codes with the too deep structures. However, all laser marks resulted in sites of slightly increased energy dissipation under reverse bias. So the proposed purely geometric SEMI specification for Data Matrix codes at the front side of the cell seems to be sufficient to exclude marking-induced efficiency losses in standard industrial solar.

Keywords: tracking, traceability, wafer identification, laser processing

1 INTRODUCTION

Traceability of single wafers through the whole PV production line becomes more important due to the expected deeper insight into the technological processes and the expected cost reduction due to an improved quality control and the process optimizations hereby enabled [1,2]. Since pure logistic tracking is not robust enough for industrial application, different procedures of wafer identification are currently developed. The suitability of laser-marked barcodes and Data Matrix codes (DMC) has already been demonstrated in recent studies at Fraunhofer ISE [2,3] and in PV industry [4]. An alternative marking method is a barcode at the edge of the wafer which is laser-marked on the brick sidewalls before cutting the wafers, the so-called brick slice code (BSC) [5]. A long position line which runs across the brick diagonal between a start line and an end line allows the position of each wafer within the brick to be determined. In all cases the code must be robust upon the solar cell manufacturing processes in terms of readability and not too deep to avoid the risk of via holes and breakage of the wafer.

In 2010 a PV Traceability Task Force started within the SEMI International Standards Program to define a global standard in which front surface markings are specified. In 2011 the standardisation procedure has been extended to the brick slice codes. The first draft of the standard for front surface marking defines a Data Matrix code with a symbol size of 14x14 cells, with a cell size of 110±10 µm, circular dots with a diameter of 90±10 µm and a depth in the range of 5 to 30 µm. The codes should be located in the middle of the wafer in a field of view with an area of 12x12 mm².

The question is whether such a purely geometric specification of the codes is sufficient to define a DMC which does not affect solar cell performance. Not defining the laser process, it has to be clarified whether the laser damage induced by standard laser processes may affect cell performance especially in the case of high-efficiency solar cells. Defining a code position on the wafer where overprinting of the code structures by the front side metallization cannot be avoided, it has to be clarified whether this increases the risk of shunts if a contact finger runs straight across the code. In this study, the impact of DMCs at the front side and BSCs at the edge of the wafer on the performance of solar cells is investigated.

2 EXPERIMENTAL

2.1 Laser marking process

To investigate the possible impact of laser marks in the active area and at the wafer edge on the electrical quality of the solar cell, both marking types are investigated on the same Cz-Si material with size of 156x156 mm². For this, one part of a Cz-Si ingot was marked at the edge with a BSC before sawing. The wafers from the unmarked part of the ingot have been partly marked with DMC and partly used as unmarked reference wafers (see Fig. 1). The wafers have been randomized after sawing to ensure that the material quality especially the ingot position has minimal impact on the results. For our experiments, we used rectangular Data Matrix codes with a symbol size of 8 x 32 cells to enable two code-grid configurations, the codes being placed on one set of samples in-between the grid fingers and on another set of samples under the grid fingers (see Fig. 1). Wafers without barcodes at the wafer edge have been marked with 4 DMCs and 400 DMCs at the front side using three different sets of laser parameters (see Fig. 1). While the groups with 4 DMC reflect the present version of the standard, the groups with 400 DMC provide a sufficient statistic of the critical elements to be investigated on a limited number of samples. In total the study consisted of 12 DMC groups with eight wafers each, one BSC group with 20 wafers and a reference group without marking with 12 wafers.

The marking of the DMCs has been done with a fully automated q-switched Nd:YVO4 IR-laser with galvanometer scanner within a marking time of 100 ms per code. The marking of the BCSs has been done with an IR-laser by Meyer Burger. Two different marking processes were used for marking the dots, the P-process and the V-process. In the P-process the dots are formed by single pulses which have to be set over each other. In this case the diameter of one dot corresponds to the laser beam diameter and slightly increases with the number of pulses due to the Gaussian profile of the laser pulse. To generate the specified code geometry several pulses were set above each other for our tests, the number of pulses being kept constant.

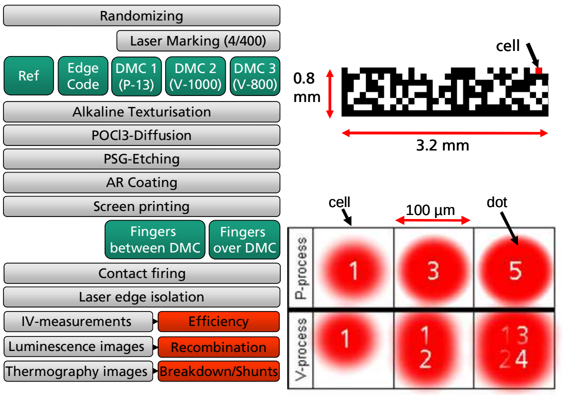

Figure 1: **(Left)** Process flow of the laser marking and the solar cell process. The target parameters of the cell characterization are given in red. **(Right)** Geometry of the DMC and the two different marking processes. In this schematic the P-process generates circular dots with the specified diameter after five laser pulses, the V-process quadratic dots after four pulses.

In the V-process several laser pulses have been placed close to each other to form one almost rectangular cell of the Matrix code, as being used in a previous study [3]. Homogeneity and depth of these V-code structures strongly depend on the pulse overlap in scribing direction, on the line overlap perpendicular to the scribing direction and on the laser power used. To generate different code depths for the reading tests the pulse overlap in scribing direction was varied in two steps. All wafers were processed in the PV-TEC pilot line using a standard industrial screen-print based Al-BSF process, as shown in Fig.1. In half of the DMC process groups the codes were overprinted by the front side metallization while being placed precisely in-between the grid fingers in the other half of the process groups, simulating a non-optimized and optimized positing of the codes. The efficiency losses have been analyzed by IV-measurements, the recombination losses by photoluminescence in different process steps and the breakdown behavior by thermography.

3 RESULTS AND DISCUSSION

3.1 Code geometry and marking characteristics

The surface structure of the codes have been analysed by SEM images after marking and after texturing. As can be seen in Fig. 2a and b, the dots of the P-13 laser-process are nearly free from any slag. The bottom of the dots is very plane. After etching no significant change in geometry has been observed. However, the grounds of the dots were textured as well. The dots marked with the V-process were surrounded by a rim and random drops of melted silicon which both are removed after etching. With a depth of around 30 µm after marking the codes P-13 and V-1000 are within the specification. After texturisation the depth remains unchanged for the P-13 code and increases for the V-1000 code up to 40 µm, which nevertheless does not violate the specification as only the geometry in the initial state after marking is addressed. However, the code V-800 with an initial depth of 110 µm is completely out of specification. After the marking process the BSC had a rim with a height of 20 µm which was reduced during the texturing to 15 µm. The flanks were very plane after etching.

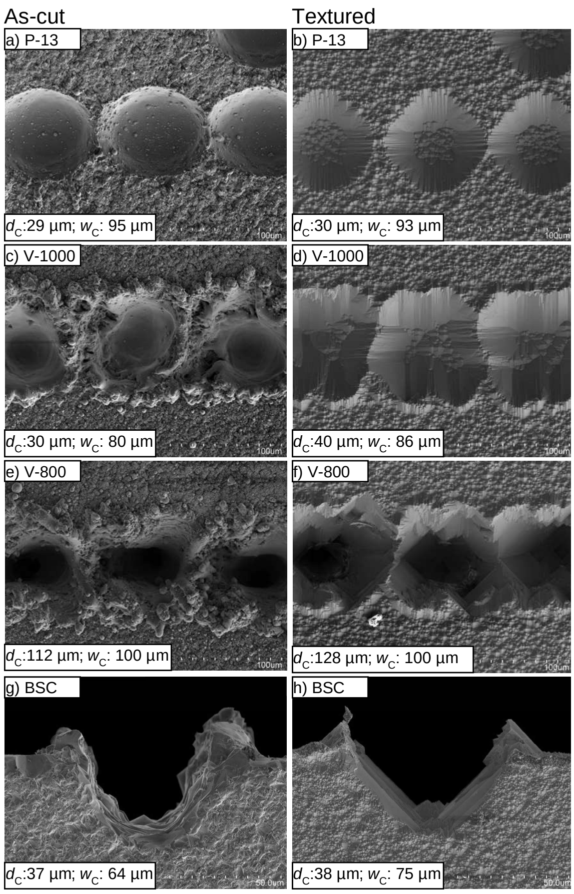

Figure 2: SEM images of three dots (a-f) and a BSC (g-h) after laser marking (left) and after texturisation (right) using different laser processes (lines). The slag around the code elements were completely removed after texturisation. The laser groove depths were measured by a confocal 3D-microscope. d_C: dot depth, w_C: dot width.

3.2 Geometry of contact fingers across code elements

On half of the solar cells with DMC the codes were overprinted by the front side metallization. The microscope images in Fig. 3 show that the codes were fully filled with paste and the finger width rose up to 210 to 230 µm at this point.

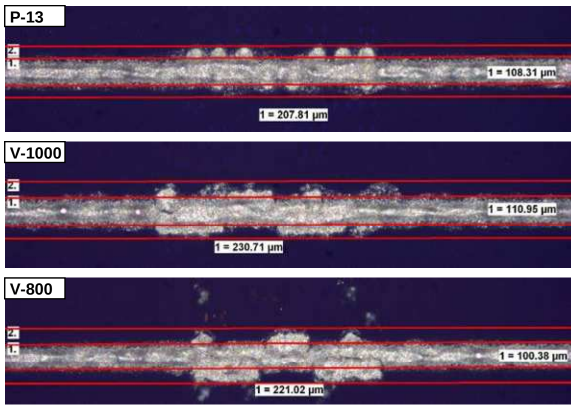

Figure 3: Microscope images of screen-printed contact fingers crossing laser-marked Data Matrix codes. An increased finger width could be observed printing over the DMCs.

Thus, finger interruptions and increased series resistances are not to be expected for these cells. However, the risk of increased paste smearing at the front side of the wafers cannot be excluded if screens are not cleaned regularly for large numbers of wafers. For mass-production, this might be a draw-back of the code position defined in the present version of the specification.

3.3 Code detection

The reading tests were performed by IOSS company. Readability has been tested in all relevant process steps, i.e., after marking, after texturisation, after anti-reflection coating and after front-side metallization. All codes were readable in all process steps. The cell geometry of the codes V-1000 and V-800 are slightly inhomogeneous and the contrast of code V-1000 is not optimal (Fig. 4), which might affect reading stability. The highest reading stability is expected for code P-13 due to the very homogeneous cell structure and the good contrast. The readability of the BSCs which are marked at the edge of the wafers was not evaluated.

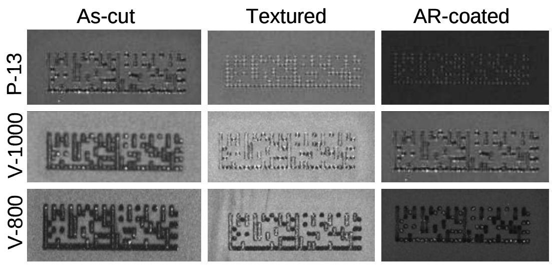

Figure 4: Code reader images from the three marking processes on Cz-Si wafers after marking, texturing and AR-coating.

3.4 IV-characteristics

Fig. 5 shows the statistics of the current voltage characteristics for the solar cells of the different process groups. The measurements have been performed directly after processing with an industrial cell tester in the PV-TEC. The average values of the reference group with an efficiency of η = 17.8 % show the quality of the applied base line process.

No significant difference in the short circuit current density J_{SC} is visible for all groups. The open circuit voltage V_{OC} is on a similar level for all groups. However, for the codes V-800, the V_{OC} scatter is significantly increased and the V_{OC} level for the group with 400 codes slightly reduced, which is caused by increased recombination losses in the deep holes of the code. Concerning the fill factor *FF*, significant reductions by more than 1%$_{abs}$ are observed for the cells with the 400 codes marked with the laser process V-800 and directly correlate to reduced shunt values R_{shunt} which is caused by the large number of deep dots (128 µm). A trend to slightly reduced fill factors is observed for the groups with overprinted DMC structures which correlate to slightly increased recombination losses J_{02}. With respect to solar cell efficiency, significant drops by 0.3%$_{abs}$ are only observed for the two V-800 groups with 400 codes in comparison to the corresponding groups with 4 codes which are marked with the same laser process.

Due to the results a reduction of the cell efficiency is not expected for an industrial standard Cz-Si solar cell process even if the code is 128 µm deep and the number of codes is limited to four. Nevertheless, the V-800 code is not recommended due to measureable efficiency loss using 400 codes and the inhomogeneous geometry of the dots.

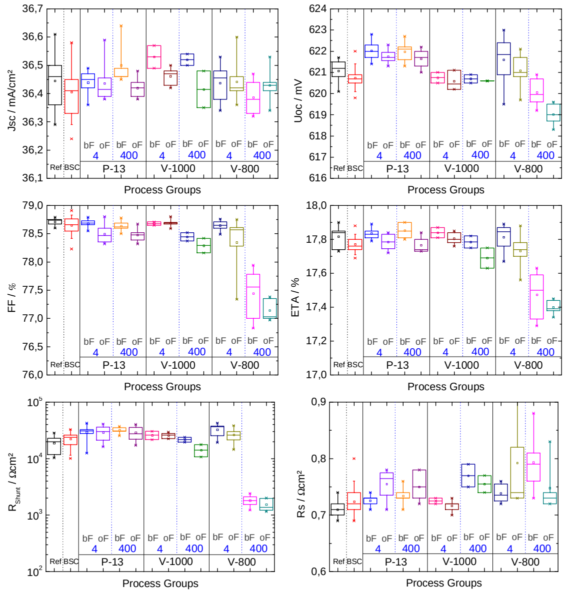

Figure 5: IV data of solar cells. Legend: bF = finger between DMC, oF = finger over DMC, 4/ 400 = number of DMCs on the cells.

3.5 Recombination losses

For the development of a laser marking process and for its process control in cell production lines it is necessary to qualify the marking process. Ideally, the process control can be done directly after the marking process. A suitable method to determine the laser damage in the wafer is the photoluminescence (PL) imaging. Fig. 6 shows the PL images of the three marking processes in four different process steps. Low intensity regions reflect regions with increased recombination. As expected, directly after marking increased recombination losses are observed for all marking processes. After texturisation the contrast variations between marked and unmarked regions shrink, which reflects the decrease in the recombination losses due to laser-damage removal.

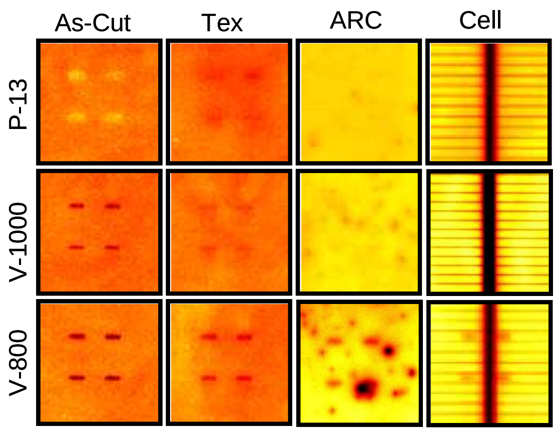

Figure 6: Photoluminescence images of Cz-Si wafers in different process steps. Recombination losses which affect the finished solar cell are detectable only after ARC and only for the V-800 code.

After antireflection coating, the PL images no more show any recombination losses for P-13 and V-1000 codes, an improvement which may arise from an annealing of the remaining laser damage during the high temperature process of emitter diffusion. Due to the partial surface passivation by the double-sided emitter diffusion and the single-sided antireflection coating, the samples are more sensitive to bulk effects than in the other process states. So a useful process control of the marking process is only possible after ARC where the laser damage which remains on the finish solar cell becomes visible.

Since the depth of a BSC mark is only 75 µm and lies out of the active area, recombination losses are not detectable on the cells marked with a BSC.

3.6 Reverse bias characteristics

If modules are partially shaded, the shaded cells operate in reverse bias conditions and dissipate energy, which may create critical hot spots if energy dissipation occurs via localized defects. In order to detect possible hot-spots, induced by the marking process, the temperature has been measured with an infrared camera, while a reverse current flew through the solar cell. To simulate module conditions the cells have been thermally insulated from the brass chuck. For this, a plastic sheet is placed between the metal chuck and the cell which is pasted with aluminium tape at the edge to ensure the rear contact. The front contact is done with contact pins, which can be seen in Fig. 7 as black vertical stripes at the top of the thermal images.

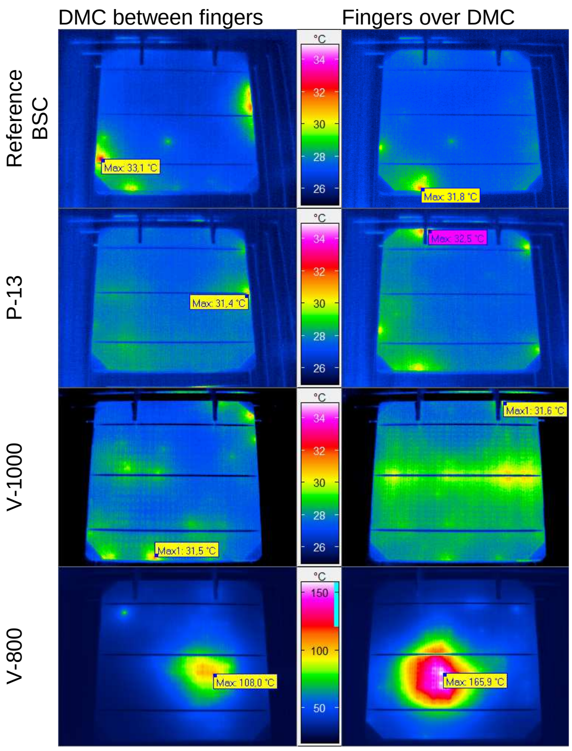

Figure 7: Infrared images measured under reverse bias conditions (-12 V) on solar cells covered with 400 DMCs between the contact fingers (left) and under the contact fingers (right) marked with the different laser processes. The top row shows a reference cell without marking (left) and a cell with BSC at the right wafer edge (right).

The voltage for reverse bias stability testing was -12 V, the temperature of the cells before measurement was 26°C. In the IR image of the unmarked reference wafer, spots with high temperatures are observed at the wafer edges. These spots originate from process-induced defects at the edges which sometimes arise at the position of the holders from the PECVD tray due to a locally reduced thickness of the AR-coating and in the corners due to wafer handling.

As the BSC structures have been introduced at the right edge of the wafer, which shows no warming in Fig. 7, the observed edge effects are process-induced (see above) and do not correlate with the BSC marking.

As no DMC structures have been introduced near the edges of the wafers, the edge effects observed in some of the DMC wafers as well have to be attributed to the process-induced edge effects (see above) and do not correlate with the DMC marking. However, as these edge defects are very efficient heat sinks, which show the highest temperatures in the IR images, they strongly reduce energy dissipation in any other spot in the cell area whenever being present. So absolute temperatures in other marking-induced spots may be higher without these background defects. Keeping this in mind, the IR images for the DMC cells should be evaluated in the following.

The wafers marked with the V-800 code show no edge effects. The maximum temperatures are reached in the area with laser marks and amount to 108°C for the cell with the DMCs in-between the fingers and to 166°C for the cell with overprinted DMCs. For this off spec laser process, the laser marks from hot spots whose efficiency increases when being overprinted. In this case module-detrimental temperatures above 150°C are reached.

In the wafers marked with the spec conform V-1000 code, a slight warming is observed in all code elements which becomes stronger if the code structures are overprinted by the contact fingers. This shows that the laser markings form sites of increased energy dissipation under reverse bias. However, as the maximum tempera-ture increase observed in the overprinted cell in a small region around the busbar only amounts to 5 K, they most likely do not form critical hot spots.

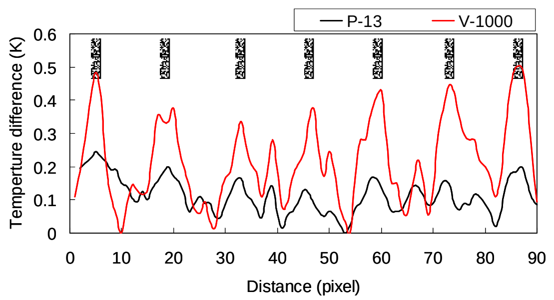

Figure 8: Profile over 7 DMCs. For the V-1000 code, the temperature in the code area is 0.5 K higher than in the interspaces. For the P-13 code, the temperature increases by only 0.2 K.

On the wafers marked with P-13 code, no warming has been detected. Since the temperature range for P-13 is set from 25 to 35°C, single codes are not visible in the images. As can be seen in Fig. 8, a profile over seven codes shows a temperature increase in the code structures of 0.2 K for code type P-13 and of 0.5 K for the code type V-1000. These small changes do not affect the performance of the solar cell. However, an impact on the reverse bias characteristic is detected with the infrared thermography for these two laser marking processes.

4 SUMMARY AND CONCLUSION

In the present work, four laser-marking processes for wafer identification have been investigated with respect to the laser-induced damage. All Data Matrix codes with a cell size of 100 µm are readable through the whole production process in which the DMCs, marked with new developed laser-process P-13 have the highest reading stability. For this marking process, the rim of a single dot is nearly free from slag, the bottom is very plane and the geometrical change after etching is negligible. IV-measurements show no significant differences in cell efficiency for all groups except the group which was marked with 400 DMCs using the laser process V-800 which produced dot depths > 100 µm.. The analysis of photoluminescence images, taken in every process step, shows that recombination losses which affect the finished solar cell are only detectable after ARC. Thermography revealed that a severe hot spot risk only arises for the V-800 code with the too deep structures. However, all laser marks resulted in sites of slightly increased energy dissipation under reverse bias.

So the proposed purely geometric SEMI specification for Data Matrix codes at the front side of the cell seems to be sufficient to exclude marking-induced efficiency losses in standard industrial solar cells of medium efficiency. But comparing the marking processes P-13 and V-1000, which are both covered by the SEMI standard with a marking depth of 30 µm, revealed that this specification allows laser processes with significant differences in reverse bias conditions and the reading quality. Thus, before launching the front side marking in a production line, an evaluation of the laser marking process with respect to the induced laser damage is very important, especially if the marking should be used for high efficiency cells.

Concerning the brick slice codes which are marked at the edge of a wafer, the readability upon the whole solar cell manufacturing process was not evaluated in this work but laser-induced damage was not detected. This opens another approach for wafer tracking in the solar industry.

5 ACKNOWLEDGEMENTS

The authors would like to thank the Meyer Burger Technology AG for brick marking and providing the wafers, IOSS for the reading tests and the whole PV-TEC staff for processing. This work has been partially supported by Meyer Burger Technology AG and the German Ministry for the Environment, Nature Conservation and Nuclear Safety (BMU) under the frame of the project QUASSIM (0325132A).

6 REFERENCES

[1] S. Rein, A. Krieg, A. Weil, G. Emanuel, M. Glatthaar, A. Grohe, R. Preu, B. Sattler, P. Lorch, K. Vayhinger: *Single-wafer tracking in PV production lines,* Proc. 23rd EU-PVSEC, Valencia, Spain, 2008, p. 1125-30

[2] P. Wawer, et al., *Every solar cell is an original: laser marking of silicon solar cells yields new opportunities in quality control*, Photovoltaics International, Tenth Edition, Fourth Quarter 2010, p 16-22

[3] A. Krieg, et al., *Wafer identification using laser marked Data Matrix codes*, Proc. 25th EU-PVSEC, Valencia, Spain (2010)

[4] U. vom Bauer, et al., *Laser marking of silicon solar cells in mass production*, Proc. 25th EU-PVSEC, Valencia, Spain (2010)

[5] S. Böckli, A. Christen., *Brick and Wafer Tracking: Requirements, Challenges and their Realisation*, to be published in Proc. 26th EU-PVSEC, Hamburg, Germany (2011)